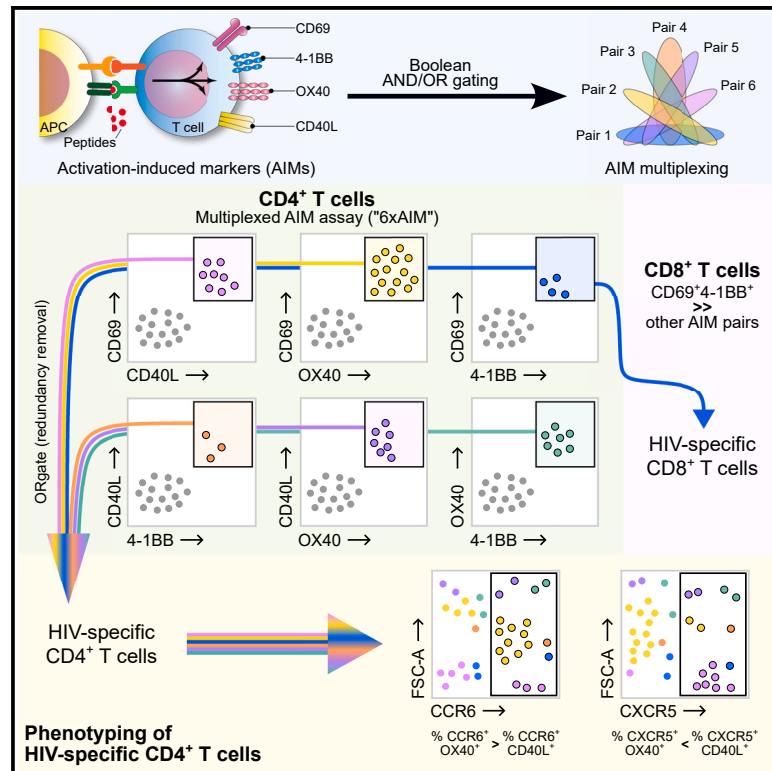**Article**

Enhanced detection of antigen-specific T cells by a multiplexed AIM assay

Graphical abstract

Authors

Audrée Lemieux, Gérémy Sannier,
Alexandre Nicolas, ..., Olivier Tastet,
Mathieu Dubé, Daniel E. Kaufmann

Correspondence

mathieu.dube.chum@ssss.gouv.qc.ca
(M.D.),
daniel.kaufmann@chuv.ch (D.E.K.)

In brief

Cytokine-independent AIM assays identify antigen-specific T cells. Lemieux et al. multiplex this approach by co-analyzing four AIMs instead of the usual two, enhancing detection of antigen-specific $CD4^+$ T cells while enabling simultaneous identification of antigen-specific $CD8^+$ T cells. This strategy reduces quantification and phenotyping biases caused by single AIM pairs.

Highlights

- The 6xAIM assay improves detection of antigen-specific $CD4^+$ T cells

- Four activation-induced markers generate six pairs that define T cell subsets

- A combination of CD69, 4-1BB, OX40, and CD40L detects $CD4^+$ and $CD8^+$ T cell responses

- This assay mitigates phenotyping biases arising through use of single AIM pairs

CellPress

Cell Reports Methods

Article

Enhanced detection of antigen-specific T cells by a multiplexed AIM assay

Audrée Lemieux,[1,2] Gérémy Sannier,[1,2] Alexandre Nicolas,[1,2] Manon Nayrac,[1,2] Gloria-Gabrielle Delgado,[1] Rose Cloutier,[1] Nathalie Brassard,[1] Mélanie Laporte,[1] Mélina Duchesne,[1] Alina Maria Sreng Flores,[1] Andrés Finzi,[1,2] Olivier Tastet,[1] Mathieu Dubé,[1,*] and Daniel E. Kaufmann[1,3,4,5,6,*]

[1]Centre de Recherche du CHUM, Montreal, QC H2X 0A9, Canada
[2]Département de Microbiologie, Infectiologie et Immunologie, Université de Montréal, Montreal, QC H2X 0A9, Canada
[3]Consortium for HIV/AIDS Vaccine Development (CHAVD), La Jolla, CA, USA
[4]Département de Médecine, Université de Montréal, Montréal, QC H2X 0A9, Canada
[5]Division of Infectious Diseases, Department of Medicine, Lausanne University Hospital and University of Lausanne, Lausanne, Switzerland
[6]Lead contact
*Correspondence: mathieu.dube.chum@ssss.gouv.qc.ca (M.D.), daniel.kaufmann@chuv.ch (D.E.K.)
https://doi.org/10.1016/j.crmeth.2023.100690

MOTIVATION Detection of circulating antigen (Ag)-specific T cells *ex vivo* is hampered by their low frequency and heterogeneity. The use of conventional cytokine-based approaches limits identification of some subsets such as T follicular helper (Tfh) cells, whose cytokines are difficult to detect. Flow cytometric activation-induced marker (AIM) assays, which work by measuring the upregulation of surface markers following T cell receptor (TCR) stimulation, are highly sensitive, cytokine-agnostic alternatives to detect Ag-specific T cells. However, they generally involve a single AIM pair. This absence of a consensus combination of molecules makes comparison between studies challenging. Many AIM pairs are also unable to detect Ag-specific CD4+ and CD8+ T cells simultaneously. Additionally, while expression of specific markers is expected to vary among T cell lineages and across antigens, side-by-side comparisons are lacking. We intend to develop an AIM assay that would mitigate these biases in the detection of infection- and vaccine-induced Ag-specific T cells.

SUMMARY

Broadly applicable methods to identify and characterize antigen-specific CD4+ and CD8+ T cells are key to immunology research, including studies of vaccine responses and immunity to infectious diseases. We developed a multiplexed activation-induced marker (AIM) assay that presents several advantages compared to single pairs of AIMs. The simultaneous measurement of four AIMs (CD69, 4-1BB, OX40, and CD40L) creates six AIM pairs that define CD4+ T cell populations with partial and variable overlap. When combined in an AND/OR Boolean gating strategy for analysis, this approach enhances CD4+ T cell detection compared to any single AIM pair, while CD8+ T cells are dominated by CD69/4-1BB co-expression. Supervised and unsupervised clustering analyses show differential expression of the AIMs in defined T helper lineages and that multiplexing mitigates phenotypic biases. Paired and unpaired comparisons of responses to infections (HIV and cytomegalovirus [CMV]) and vaccination (severe acute respiratory syndrome coronavirus 2 [SARS-CoV-2]) validate the robustness and versatility of the method.

INTRODUCTION

Antigen (Ag)-specific CD4+ and CD8+ T cells play a critical role in immune responses against viral infections.[1–3] While CD8+ T lymphocytes kill cells infected with intracellular pathogens via their cytotoxic activity, CD4+ T cells produce cytokines that modulate the functions of other cells. CD4+ T cells include subsets like T follicular helper (Tfh) cells, whose interaction with B cells is critical to regulate the antibody response;

Th1, constituting important immune responses against viruses and other intracellular pathogens; and Th17 and Th22, implicated in mucosal immunity.[4–6] However, the direct detection of circulating Ag-specific T cells *ex vivo* is hampered by both their relatively low frequency and their heterogeneity.[7,8] Typically, pathogen-specific T cells are detected with conventional cytokine-based approaches such as intracellular cytokine staining (ICS) or enzyme-linked immunosorbent spot (ELISpot).[9] However, their use can bias the sampling of

subsets like Tfh cells, whose cytokines are more difficult to detect.[7,10,11]

To overcome these limitations, the flow cytometric activation-induced marker (AIM) assay, which measures the upregulation of selected surface markers following T cell receptor (TCR) stimulation after encounter with the cognate Ag, was developed.[7,12–14] AIM assays rely on molecules that are quickly upregulated at the cell surface. In contrast to soluble cytokines, these membrane-associated markers do not need to be chemically trapped inside the cells, as done in ICS and related methods, thus allowing identification and, for specific downstream analyses, sorting of live cells. Moreover, while the AIM assay is a functional assay, as it requires the activation of the cell through its TCR, it is a robust and highly sensitive alternative for cytokine-independent detection of Ag-specific T cells.[7,12,13,15] In the past, single AIMs,[8,16–18] or single pairs of AIMs including, but not restricted to, CD40L$^+$CD200$^+$,[18] OX40$^+$CD25$^+$,[7,14,19,20] CD69$^+$CD40L$^+$,[7,14,20–24] CD69$^+$OX40$^+$,[14,25,26] or CD69$^+$4-1BB$^+$,[14,24,26–29] have been used to detect T cells of different specificities. These molecules were specifically chosen for their known induction on activated T cells after TCR activation. However, there are limitations to using single AIM pairs: the absence of a consensus combination of molecules across the literature makes it difficult to compare between studies. The commonly used CD69$^+$CD40L$^+$ assay, which works well on blood samples, cannot be used in lymphoid tissues, as CD69 is physiologically expressed at high levels on germinal center (GC) Tfh cells.[15] Many pairs of AIMs are also unable to detect Ag-specific CD4$^+$ and CD8$^+$ T cells simultaneously.

Here, we assessed in depth a multiplexed version of an AIM assay used in recent studies.[30–34] This assay integrates and co-analyzes four AIMs—CD69, 4-1BB (CD137), OX40 (CD134), and CD40L (CD154)—rather than two. We examined if this assay could overcome the possible biases related to the selection of a single pair of AIMs. We assessed the efficiency of the approach to capture HIV-specific CD4$^+$ and CD8$^+$ T cells and examined the additional coverage provided by each AIM pair. We evaluated whether the AIMs were preferentially expressed on CD4$^+$ T cells expressing defined lineage markers. We compared the observed profiles to T cell responses specific for another chronic virus (cytomegalovirus [CMV]), as well as those induced by severe acute respiratory syndrome coronavirus 2 (SARS-CoV-2) vaccination.

RESULTS

The multiplexed AIM assay improves detection of HIV- and CMV-specific CD4$^+$ T cells

We first studied the ability of the multiplexed AIM assay to profile HIV-specific CD4$^+$ and CD8$^+$ T cell responses. We examined the co-expression patterns of CD69, 4-1BB, OX40, and CD40L on T cells after a 15 h stimulation with HIV Ags.[34] The 15 h stimulation was selected as a compromise for the different time frames used for single-pair assays relying on CD40L (9 h being optimal, as it is upregulated early)[7,35] and OX40 (up to 24 h being optimal).[7,36,37] We focused on a cohort of 16 people with HIV (PWH) on suppressive antiretroviral therapy (ART) with <40 plasma viral RNA (vRNA) copies/mL (Table S1). The four activa-

tion markers can be combined to form six different AIM pairs post hoc to infer Ag specificity (Figures 1A, S1A, and S1B). AIMs, as functional molecules, may or may not be expressed by certain Ag-specific T cells. We hypothesized that combining multiple pairs would provide a more representative sampling of Ag-specific CD4$^+$ and CD8$^+$ T cells. On the other hand, CD4$^+$ and CD8$^+$ T cells are often polyfunctional[20,38–40] and can express more than one AIM pair, with sizable overlap between cell subpopulations. To measure the total Ag-specific responses, we therefore used an AND/OR Boolean combination gating strategy ensuring that AIM$^+$ cells are counted only once. In the example provided in Figure 1B about CD69$^+$CD40L$^+$ and CD69$^+$OX40$^+$ CD4$^+$ T cells, the combined signal would be 0.75% (Boolean OR gating) and not 1.05% (sum of frequencies), as there was a 0.30% redundancy between those two pairs.

We used the multiplexed AIM assay (henceforth termed "6xAIM") to broadly detect HIV-specific CD4$^+$ and CD8$^+$ T cells, as done previously.[21,22,41] We measured AIM$^+$ T cell responses following an *ex vivo* 15 h stimulation of cryopreserved peripheral blood mononuclear cells (PBMCs) with overlapping peptide pools spanning the HIV Gag, Pol, Envelope (Env), and Nef proteins (Figure 1C). To examine whether the patterns of AIM expression observed for HIV-specific T cell responses were specific to this pathogen or generalizable to other viral infections, we measured in parallel the responses against CMV, a life-long infection highly prevalent in PWH.[42] As CMV-specific CD4$^+$ T cells are known to be more terminally differentiated,[43] we hypothesized that the hierarchy of AIM pairs might differ from HIV-specific CD4$^+$ T cells. We studied the same cohort of PWH, excluding one donor who was negative for CMV (Table S1). This allowed paired, intrahost comparisons of CD4$^+$ and CD8$^+$ T cells specific for two viruses (Figure 1D). As CMV is a large virus encoding numerous proteins, we focused on responses to the lower matrix protein pp65. The variations between technical replicates (Figure S1C) and independent experiments (Figure S1D) were low, indicating good reproducibility of the AIM assay.

The false positive rate is an inherent limitation of any functional assay. Bystander activation was found to be minimal in standard AIM assays relying on OX40$^+$CD25$^+$ and CD69$^+$CD40L$^+$.[7] We tested if the integration of multiple AIM pairs increased the false positive signal due to bystander activation. We collected supernatants from a primary AIM assay (AIM #1) conducted on Gag-stimulated PBMCs from ART participants and then performed a second AIM assay (AIM #2) using the conditioned supernatants to activate sentinel T cells from an HIV-naïve participant (Figure S1E). The signal observed in AIM #2 remained similar to the background in AIM #1, indicating minimal bystander activation in this setting (Figure S1F).

We subtracted the background signal (values of unstimulated conditions, used as a negative control)[7,13,17,19,21–23,41] to obtain net responses (Figures S2A and S2B). To assess the "total" HIV-specific responses in the ART-suppressed cohort, we then summed up the net Gag-, Pol-, Env-, and Nef-specific responses (Figure S2A). We compared the magnitude of HIV-specific T cell responses detected by each AIM pair as well as the 6xAIM multiplexed combination of the six AIM pairs (Figure 2A). Matched comparisons using the Friedman test with Dunn's correction
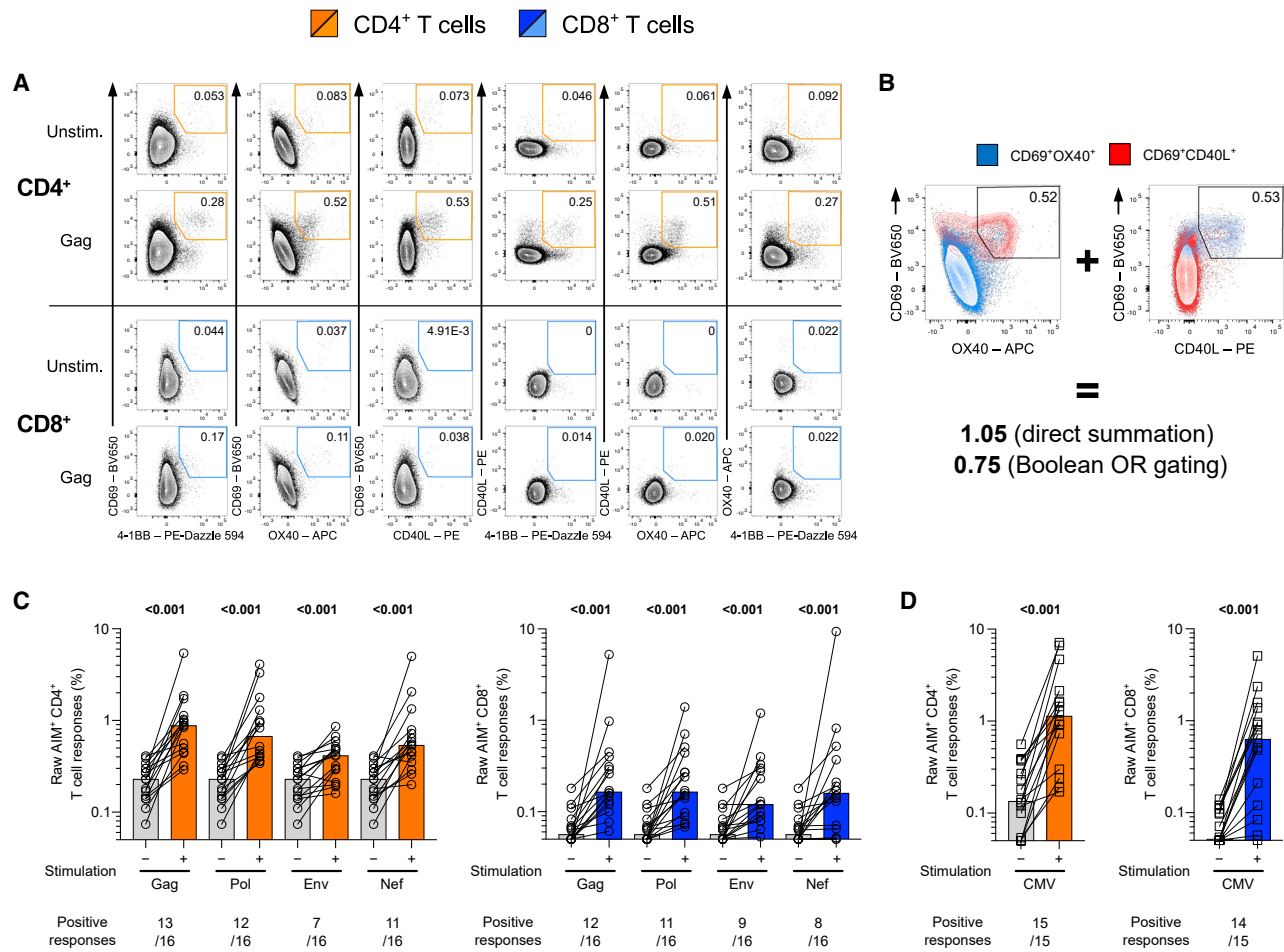
Figure 1. Quantification of Ag-specific CD4⁺ and CD8⁺ T cell responses using Boolean OR gating

(A) Representative FACS plots depicting the multiplexed (6xAIM) strategy to identify Ag-specific CD4⁺ (orange gate) and CD8⁺ (blue gate) T cells. For simplicity, the example focuses on the HIV Gag stimulation.

(B) FACS plots illustrating the AND/OR Boolean gating strategy. For simplicity, the example focuses on the AIM pairs CD69⁺OX40⁺ (blue population) and CD69⁺CD40L⁺ (red population).

(C and D) Raw frequencies of (C) AIM⁺ CD4⁺ and CD8⁺ T cell responses following an *ex vivo* 15 h stimulation of PBMCs with a pool of HIV Gag, Pol, Envelope (Env), or Nef peptides, or (D) following stimulation with HCMVA pp65 peptides. PBMCs were left unstimulated as a control (gray bars). Numbers of responders reaching >2× over the unstimulated condition are written below the histograms for each stimulation. The median 6xAIM values and Wilcoxon tests are shown. (C) n = 16 ART participants; (D) n = 15 CMV⁺ ART participants.

revealed several statistically significant differences in these magnitudes (Figure 2A). For HIV-specific CD4⁺ T cells, the CD69⁺OX40⁺ and OX40⁺4-1BB⁺ responses were of larger magnitudes, while the CD40L⁺4-1BB⁺ combination captured the least cells. Only subtle differences were observed for CMV responses when single AIM pairs were compared (Figure 2B). The multiplexed 6xAIM quantification consistently provided higher detection of HIV- and CMV-specific CD4⁺ T cell responses compared to single AIM pairs. In contrast to Ag-specific CD4⁺ T cells, no such hierarchy existed for CD8⁺ T cells. The multiplexed AIM⁺ CD4⁺ T cell response was strongly dominated by the CD69⁺4-1BB⁺ combination. The detection provided by CD69⁺4-1BB⁺ was equivalent to the 6xAIM strategy (Figures 2A and 2B).

Direct side-by-side comparisons with AIM pairs that have been extensively used in the past to detect Ag-specific CD4⁺

T cells, i.e., CD69⁺OX40[7,14,20–24] and CD69⁺CD40L⁺[14,25,26] (Figures 2C and S2C), further demonstrated the benefit of the 6xAIM in terms of the magnitude of responses detected. AIM⁺ responses were, respectively, 1.9 and 3.2 times higher with the 6xAIM approach and reached significance with Wilcoxon signed-rank tests. Despite the different kinetics of AIM markers, the 6xAIM yielded the highest CD4⁺ T cell responses throughout various stimulation durations commonly employed in standard AIM assays, such as 9,[7,21–23] 15,[30–34] and 24 h[18,19,25,27,28] (Figure S2D). The 6xAIM analysis did not increase the false positive signal due to bystander activation (Figure S2E).

Predictably, integrating multiple AIM pairs led to some increase in background signal (Figure S2C). We next assessed if the enhanced detection of Ag-specific CD4⁺ T cells achieved by the 6xAIM came at the expense of a proportionally higher

Not >2x over unstim (no response)   >2x over unstim (positive responses)
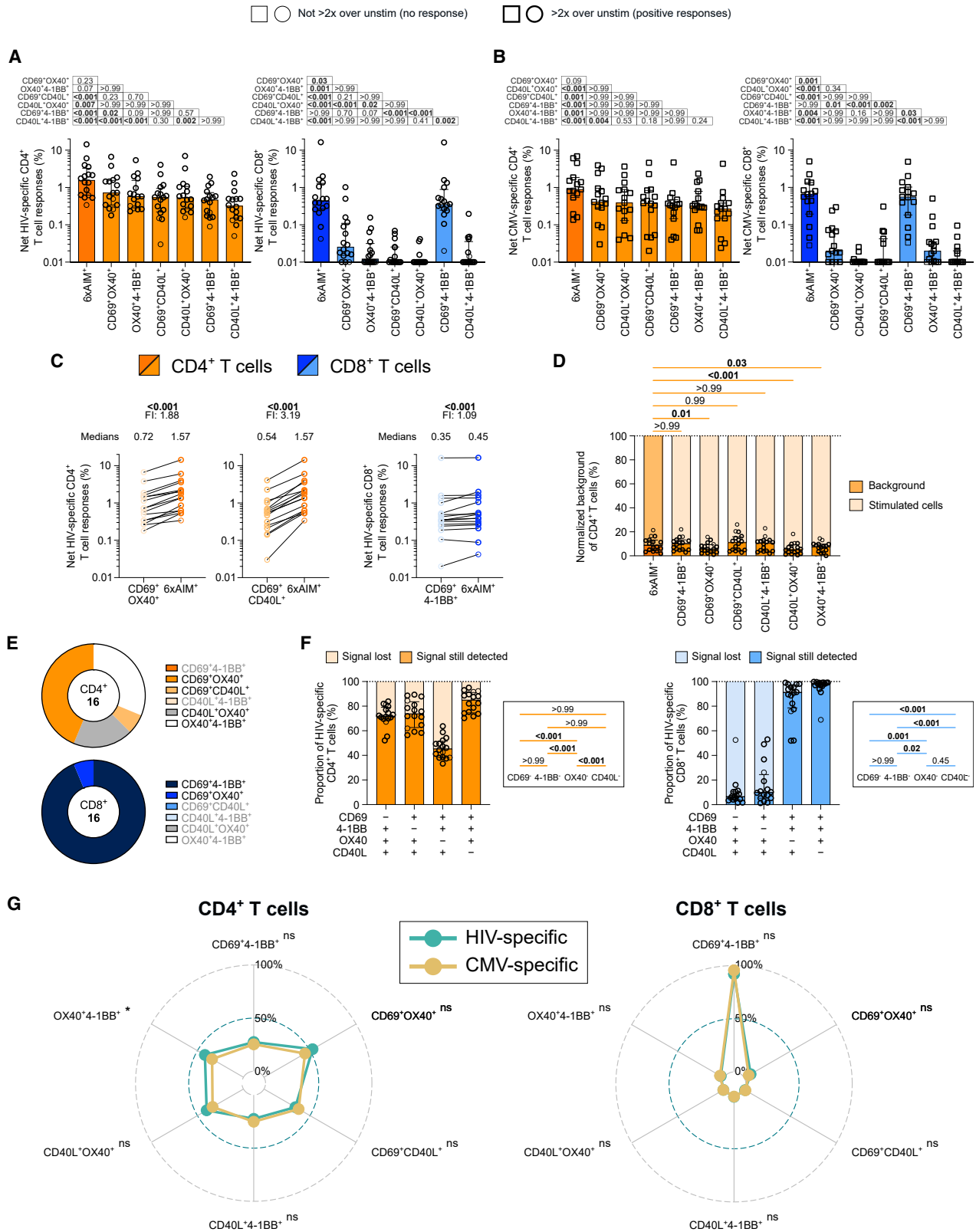
(legend on next page)

background. We calculated the ratio of the signal in the unstimulated vs. Ag-stimulated conditions (Figure 2D). For individual pairs, the background signal constituted a median of 5%–11% of the stimulated signal. The median background level for 6xAIM was within that range, at 9%. Therefore, the 6xAIM approach generates a background signal proportionally equivalent to standard single AIM pairs.

Different pairs of AIMs can identify overlapping Ag-specific T cell populations. To map this redundancy, we generated combination gates, creating 64 ($2^6 = 64$) theoretical combinations (Figure S2F). Each entry refers to a combination of pairs, for example a population identifiable by all six pairs of AIMs (indicated by "i" in Figure S2F), or a population only identifiable by CD69$^+$4-1BB$^+$ (indicated by "ii"). Of all these combinations, only a handful represented sizable fractions of HIV-specific CD4$^+$ and CD8$^+$ T cells. For instance, none of the HIV-specific CD4$^+$ T cells exhibited exclusive positivity for CD40L$^+$4-1BB$^+$ and CD69$^+$OX40$^+$, whereas 20% were positive for OX40$^+$4-1BB$^+$ exclusively, without any other pair being detected. Therefore, co-expression of AIMs followed constrained patterns.

The AIM pair combinations detecting the largest fraction of the 6xAIM$^+$ HIV-specific CD4$^+$ T cell population varied from donor to donor (Figure 2E). Therefore, relying on a single AIM pair can lead to underestimation of the T helper responses. In contrast, the CD69$^+$4-1BB$^+$ combination dominated HIV-specific CD8$^+$ T cells, with a single exception.

We next assessed the contribution of each individual marker to the global detection of HIV- and CMV-specific T cells. To accomplish this, we iteratively removed them one by one from the multiplexed analysis and calculated the proportion of the signal consequently lost (Figures 2F and S2G). Because of partial overlap and co-expression, we still achieved good detection of Ag-specific CD4$^+$ T cells in the combinations missing one marker. Removal of OX40 was significantly more detrimental than the removal of the other AIMs, showing that there is less redundancy and co-expression for this marker. In contrast, both CD69 and 4-1BB were required for the identification of HIV- and CMV-specific CD8$^+$ T cells.

As the 6xAIM represented the maximum responses obtained, we also normalized the virus-specific responses to their respective 6xAIM values and found that patterns of detection were relatively similar between HIV- and CMV-specific CD4$^+$ and CD8$^+$ T cells, respectively (Figures 2G and S2H). These results indicate that the expression patterns of individual markers and marker pairs within the multiplexed AIM assay are quite consistent among T cell responses to two very different chronic viruses. These data also suggest that the risk of introducing biases by focusing on a single AIM pair to compare responses to different pathogens is probably small within the same group of participants.

These results indicate that a multiplexed AIM panel containing the markers CD69, 4-1BB, OX40, and CD40L allowed simultaneous detection of Ag-specific CD4$^+$ and CD8$^+$ T cells. The Boolean 6xAIM analysis increased the detection of HIV- and CMV-specific CD4$^+$ T cells compared to single-pair assays, while CD8$^+$ T cells were readily identified by the CD69$^+$4-1BB$^+$ combination.

CD69, 4-1BB, OX40, and CD40L are differentially expressed on HIV-specific CD4$^+$ T cell subsets

HIV-specific CD4$^+$ T cells defined by the 6xAIM strategy expressed different levels of AIMs, with larger fractions of CD69$^+$ and OX40$^+$ cells compared to 4-1BB and CD40L (Figures 3A and S3A). AIMs are functional molecules that may be differentially expressed depending on the CD4$^+$ T cell subsets. Therefore, we assessed whether these differences in expression could impact the profile of the HIV-specific CD4$^+$ T cell subsets detected. We phenotyped AIM$^+$ HIV-specific CD4$^+$ T cells using a high-parameter fluorescence-activated cell sorting (FACS) panel (Table S2) based on expression of chemokine receptors that are preferentially—but not exclusively—expressed by defined lineages: CXCR5 for Tfh, CXCR3 for Th1, CCR6 for Th17/Th22, an inhibitory checkpoint (PD-1), and activation markers (CD38, HLA-DR). The uniform manifold approximation and projection (UMAP) algorithm[44] was used to illustrate the distribution of HIV-specific CD4$^+$ T cell populations (Figure 3B). These populations were clustered with the Phenograph algorithm,[45] which identified 12 distinct populations based on their relative marker

Figure 2. The multiplexed 6xAIM assay improves detection of HIV- and CMV-specific CD4$^+$ T cells
(A) Net HIV-specific CD4$^+$ and CD8$^+$ T cell responses. The net HIV Gag, Pol, Env, and Nef responses were summed to assess the "total" HIV-specific responses.
(B) Net CMV-specific CD4$^+$ and CD8$^+$ T cell responses.
(C) Comparisons between the net responses of the 6xAIM strategy and benchmark AIM pairs to detect Ag-specific CD4$^+$ and CD8$^+$ T cell responses. Medians, median fold increases (FIs), and Wilcoxon tests are shown.
(D) Proportion of background signal in HIV Ag-stimulated conditions. The Ag-stimulated conditions are normalized to 100% to better represent the autologous unstimulated signal. Light colors represent the total of stimulated cells; dark colors represent the background.
(E) Donut charts depicting the proportion of participants for whom each AIM pair yielded the highest magnitude of HIV-specific CD4$^+$ and CD8$^+$ T cell responses.
(F) Individual contributions of each AIM marker for the detection of HIV-specific CD4$^+$ and CD8$^+$ T cell responses. The detection levels were normalized to the value yielded by the 6xAIM. Light colors represent the signal lost when the indicated AIM marker was removed from the analysis; dark colors represent the residual signal still detected.
(G) Spider charts depicting the comparisons between the normalized amplitudes of the net HIV- (teal) and CMV-specific (amber) CD4$^+$ and CD8$^+$ T cell responses. Within each cohort, responses were normalized to their 6xAIM values. Medians and Wilcoxon tests are shown for each pair (see also Figure S2H). *p < 0.05, **p < 0.01, and ***p < 0.001. Matched donors who had at least one HIV stimulation and the CMV stimulation reaching >2× over the unstimulated conditions were kept. For CD4$^+$ and CD8$^+$ T cells, n = 13 CMV$^+$ ART-matched participants.
(A and B) The 6xAIM and individual AIM pairs are ranked in decreasing order of the median, based on their respective CD4$^+$ T cells. The tables above the graphs represent the pairwise multiple comparisons performed using the Friedman test with Dunn's post hoc test. (D and F) Pairwise multiple comparisons were performed using the Friedman test with Dunn's post-hoc test. (A, B, D, and F) The bars represent medians ± interquartile ranges. Thicker borders represent donors who had at least one HIV stimulation, or had the CMV stimulation, reaching >2× over the unstimulated conditions. (A, C, and D–F) n = 16 ART participants; (B) n = 15 CMV$^+$ ART participants.
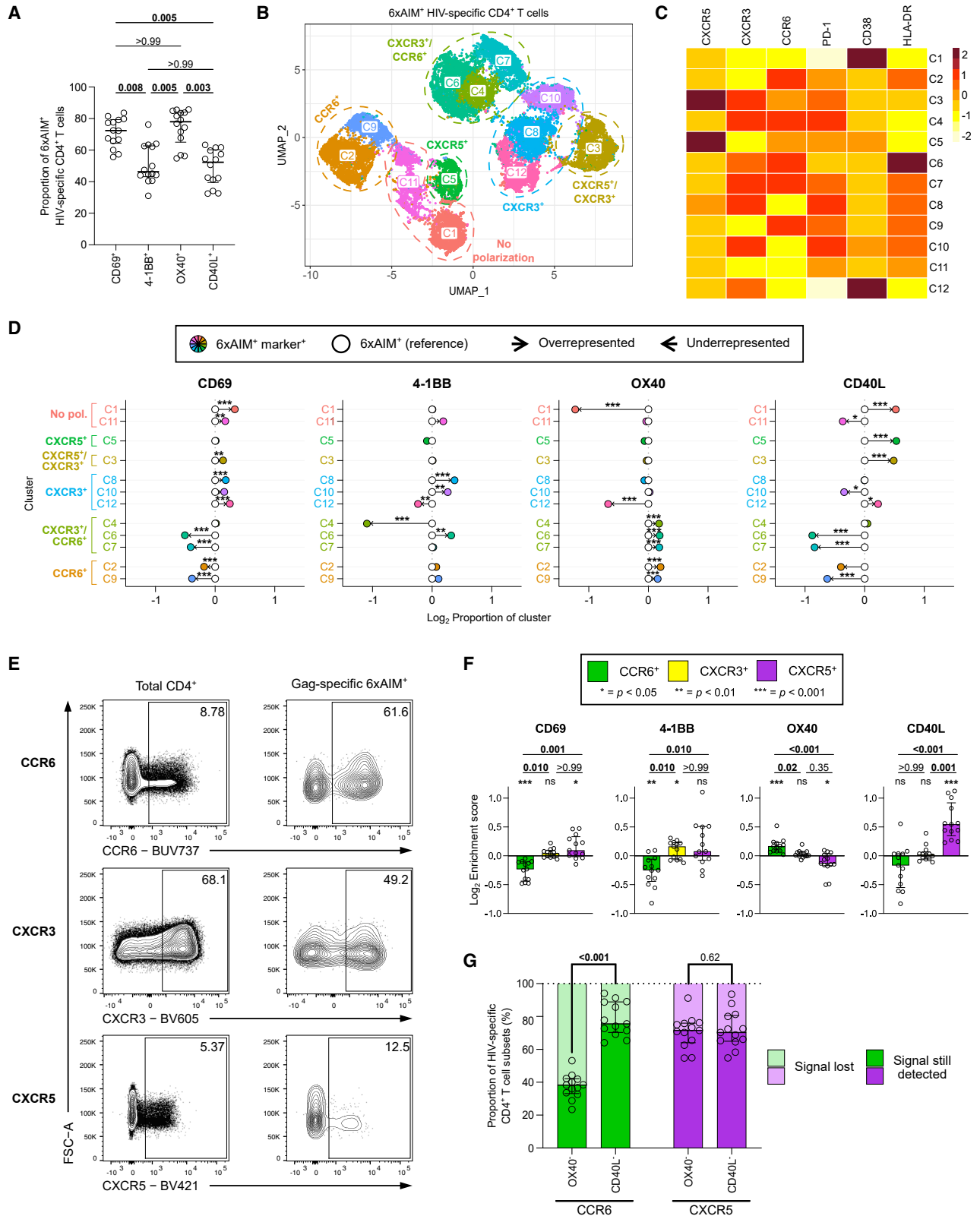
expression (Figures 3C and S3B). These populations could be further grouped in "superclusters" driven by their chemokine receptor expression (Figure 3B).

We next tested if individual AIMs were particularly associated with certain polarization markers. Univariate gatings were applied to identify, within the total 6xAIM+ population, Ag-specific cells expressing CD69, 4-1BB, OX40, and/or CD40L (Figure S3A). The phenotypes of AIM+ CD69+, AIM+ 4-1BB+, AIM+ OX40+, and AIM+ CD40L+ CD4+ T cell subpopulations were compared to the global 6xAIM+ CD4+ T cells, which served as the reference parental population (Figure S3C). These data are also summarized in Figure 3D, where relative enrichments were calculated for each phenotypic clusters in CD69+, 4-1BB+, OX40+, and CD40L+ Gag-specific CD4+ T cells compared to the reference 6xAIM+ Gag-specific population. The relative frequency of each of these populations varied depending on the AIM expressed. OX40+ Gag-specific cells were the most comparable to the reference 6xAIM+ CD4+ T cell population. Only C1 and C12 strongly diverged, being underrepresented in OX40+ Gag-specific cells. Yet, CCR6+ clusters (C2, C4, C6, C7, and C9) were modestly but consistently enriched in this subpopulation. In contrast to OX40, the AIM+ CD69+ population tended to be underrepresented in CCR6+ clusters (C2, C6, C7, and C9) but enriched in CXCR3+ clusters (C3, C8, and C12). Differences were more profound for CD40L, as clusters with Tfh-like signatures (C3 and C5) were significantly overrepresented, to the detriment of Th17/Th22-like clusters (C2, C6, C7, and C9). Phenotypic biases were also observed in AIM+ 4-1BB+ cells, as C4 was largely decreased, whereas C6, C8, and 10 were overrepresented. Thus, individual AIMs preferentially identify different subsets of Ag-specific CD4+ T cells.

We validated these observations with focused univariate analyses of chemokine receptor expression (Figure 3E). We examined Gag-specific responses, as we found strong AIM+ CD4+ T cell responses against this antigen (Figure 1C). We compared the expression of CD69, 4-1BB, OX40, and CD40L in Gag-specific CCR6+, CXCR3+, and CXCR5+ CD4+ T cells to their expression in the parental AIM+ Gag-specific CD4+ T cell population

and calculated enrichment scores (Figure S3D). The pattern of AIM expression in CXCR3+ cells was similar to the parental population (Figures 3F and S3E). Consistent with the unsupervised analyses, we found that CD40L was preferentially expressed in the CXCR5+ population to the detriment of CCR6+ cells, while we saw the opposite for OX40, which was slightly enriched in Th17/Th22-like cells. We next tested whether the removal of OX40 or CD40L would affect the detection of HIV-specific CXCR5+ and CCR6+ cells (Figure 3G). Removal of CD40L resulted in a median 24% decrease in HIV-specific CCR6+ CD4+ T cells. The loss of detection was significantly exacerbated when OX40 was excluded instead, with a median 62% decrease. In contrast, removal of either OX40 or CD40L resulted in a similar median decrease (28% vs. 30%) of HIV-specific CXCR5+ CD4+ T cells, despite the enrichment of CD40L in Tfh cells.

We next verified if the 6xAIM could capture subtle Ag-specific phenotypic skewing by comparing Gag- and CMV-specific CD4+ T cells (Figure S3F). The 6xAIM approach captured the previously reported[22] higher proportions of CXCR3+ and CXCR5+ cells in the total Gag-specific CD4+ T cell population as compared to CMV pp65-specific CD4 T+ cells (Figure S3G).

These results show that the sampling and phenotyping of HIV-specific CD4+ T cells may vary depending on the pairs of AIMs selected. Integrating multiple AIMs mitigates these variations. However, a certain degree of redundancy exists between the AIMs, and the removal of a single AIM molecule still allows the detection of all unsupervised clusters.

Infection-specific (HIV) and vaccine-induced (SARS-CoV-2) responses are detected by the same AIM pairs

Finally, to test the versatility of our approach, we examined the multiplexed AIM responses in a cohort of 23 healthcare workers (HCWs) three weeks after the second dose of SARS-CoV-2 mRNA vaccines (Figure S4A). These participants were vaccinated according to a long 16 week interval regimen as previously published by our group (Table S1).[31–33] We next compared the features of the infection-induced HIV-specific T cells in PWH to those of vaccine-induced SARS-CoV-2

Figure 3. CD69, 4-1BB, OX40, and CD40L are differentially expressed on HIV-specific CD4+ T cell subsets
Phenotypic analysis of HIV-specific CD4+ T cell responses.
(A) Proportion of 6xAIM+ HIV-specific CD4+ T cells expressing CD69, 4-1BB, OX40, and CD40L in univariate analyses (see also Figure S3A for gating strategy).
(B) Multiparametric global UMAP representation of 6xAIM+ HIV-specific CD4+ T cells. The colors identify 12 populations clustered by unsupervised analyses and labeled on the UMAP. These populations could be further grouped in "superclusters" driven by their chemokine receptor expression. Clusters that were not polarized toward CCR6+, CXCR3+, or CXCR5+ T cells were classified as "no polarization."
(C) Heatmap summarizing the mean fluorescence intensity (MFI) of each loaded parameter.
(D) Relative frequency of each identified cluster within 6xAIM+ HIV-specific CD4+ marker+ T cell subpopulations (colored dots) compared to within the reference parental 6xAIM+ cells (white dots). Arrows pointing to the right indicate that a population is overrepresented in the HIV-specific population compared to the reference CD4+ T cells, while arrows pointing to the left indicate an underrepresentation. Medians and only significant results with the Wilcoxon tests (see also Figure S3C) are shown. *p < 0.05, **p < 0.01, and ***p < 0.001.
(E) Example of univariate CCR6+, CXCR3+, and CXCR5+ gatings on total and HIV Gag-specific CD4+ T cell populations.
(F) Enrichment scores of the AIMs in the Gag-specific CD4+ CCR6+ (green), CXCR3+ (yellow), and CXCR5+ (purple) T cell populations. The scores were calculated by dividing, for each individual AIM, the Gag-specific CD4+ phenotype+ population by the Gag-specific CD4+ population, irrespective of the polarization (see also Figure S3D). Wilcoxon tests (see also Figure S3E) are shown. *p < 0.05, **p < 0.01, and ***p < 0.001.
(G) Proportion of HIV-specific CCR6+ and CXCR5+ CD4+ T cells still detected after ad hoc removal of the indicated AIM molecules. The values were normalized to those of the 6xAIM. Wilcoxon tests are shown.
(A, F, and G) Medians ± interquartile ranges are shown. (A and F) Pairwise multiple comparisons were performed using the Friedman test with Dunn's post-hoc test. (D and F) The graphs are on a log$_2$ scale. To avoid contaminating phenotype profiling with excessive background, donors who had at least one HIV stimulation (A–D) or the HIV Gag stimulation (F and G) reaching >2× over the unstimulated condition were kept. (A–D) n = 14 ART participants; (F and G) n = 13 participants.
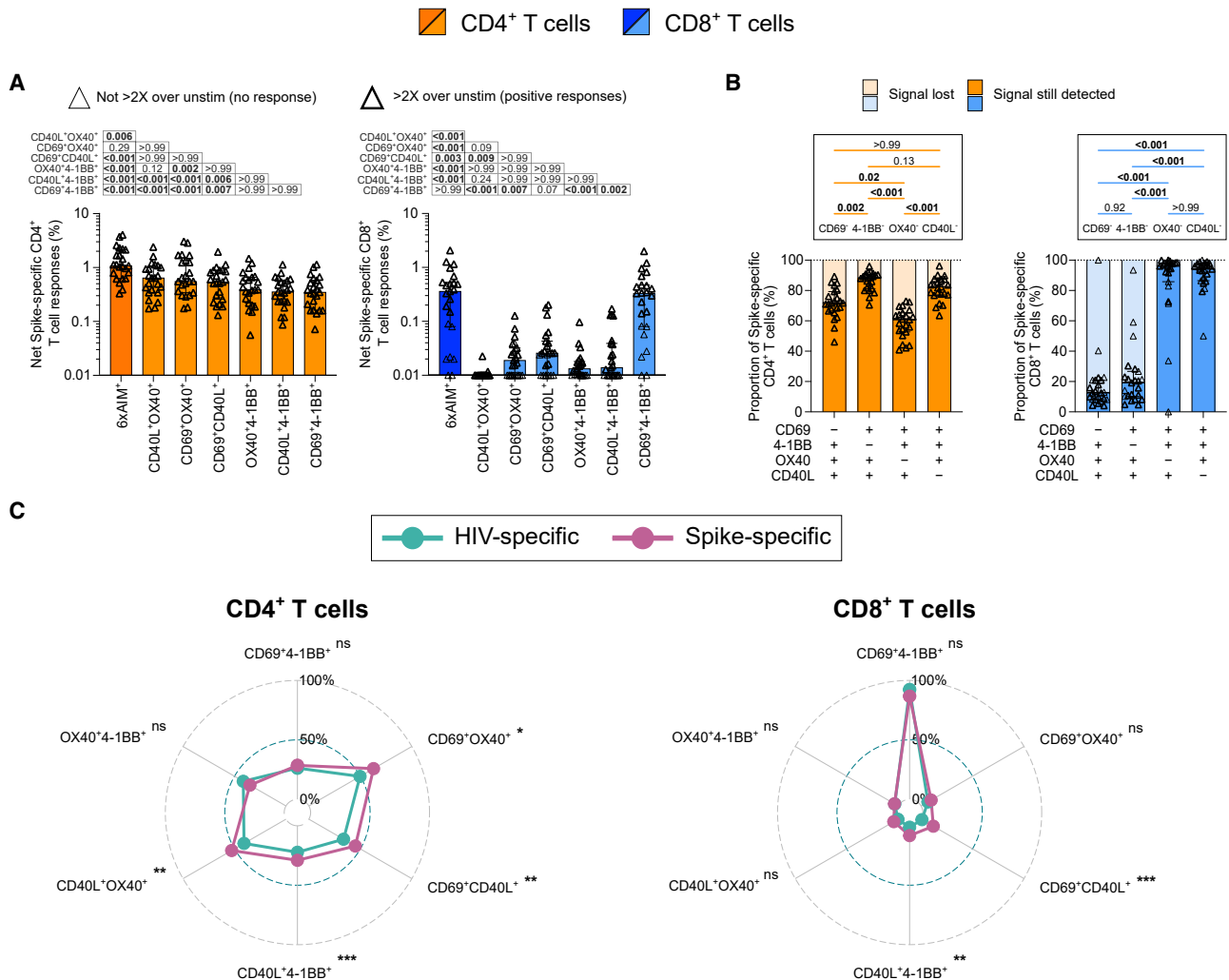
Figure 4. Infection-specific (HIV) and vaccine-induced (SARS-CoV-2) responses are detected by the same AIM pairs

(A) Net SARS-CoV-2 Spike-specific CD4+ (orange) and CD8+ (blue) T cell responses. The 6xAIM and individual AIM pairs are ranked in decreasing order of the median, based on the CD4+ T cells. The tables above the graphs represent the pairwise multiple comparisons performed using the Friedman test with Dunn's post hoc test.

(B) Individual contributions of each AIM marker for the detection of Spike-specific CD4+ (left) and CD8+ (right) T cell responses. The detection levels were normalized to the value yielded by the 6xAIM. Light colors represent the signal lost when the indicated AIM marker is removed from the analysis; dark colors represent the residual signal still detected. Pairwise multiple comparisons were performed using the Friedman test with Dunn's post-hoc test.

(C) Spider charts depicting the comparisons between the normalized amplitudes of net HIV- (teal) and Spike-specific (lavender) CD4+ and CD8+ T cell responses. Within each cohort, responses were normalized to their 6xAIM values. Medians and Mann-Whitney tests are shown for each pair (see also Figure S4D). *p < 0.05, **p < 0.01, and ***p < 0.001. Donors who had at least one HIV stimulation reaching >2× over the unstimulated conditions were kept, as well as those whose Spike stimulation reached the same threshold. For CD4+ T cells, n = 14 ART participants and n = 23 SARS-CoV-2-vaccinated participants; for CD8+ T cells, n = 15 ART participants and n = 16 SARS-CoV-2-vaccinated participants.

(A and B) The bars represent medians ± interquartile ranges. Thicker borders represent donors whose stimulation reached >2× over the unstimulated conditions. n = 23 SARS-CoV-2-vaccinated participants.

Spike-specific T cells in HCWs (Figures S4B and S4C). Consistent with our observations on HIV-specific T cell responses, we found that the 6xAIM approach provided more robust measures of Spike-specific CD4+ T cell responses (Figure 4A). Moreover, OX40 (CD4+) was still the most important AIM molecule for Spike-specific T cell detection (Figure 4B). Both CD69 and 4-1BB were essential to detect Spike-specific CD8+ T cells (Figures 4A and 4B).

We next tested whether individual AIM pairs provided similar estimations of Ag-specific CD4+ and CD8+ T cell responses in different cohorts. For this comparative purpose, we normalized the data based on the 6xAIM, which provided the highest detection levels in both cohorts (Figures 4C and S4D). Despite some differences, the overall pattern of detection was similar between the two cohorts. In CD8+ T cells, the CD69+4-1BB+ pair was equivalently efficient at detecting Ag-specific cells. These data

CellPress
OPEN ACCESS

indicate that the use of a single AIM pair does not introduce major cohort-based biases in quantifications.

DISCUSSION

In this study, we provide a new approach to enhance the sensitivity of the AIM assay by multiplexing AIM markers that have been validated in previous studies. We tested the robustness of a multiplexed AIM assay that combined CD69, 4-1BB, CD40L, and OX40 and comprehensively compared this integrated approach to individual AIM pairs. The multiplexed AIM approach consistently detected higher magnitudes of net Ag-specific CD4^{+} T responses than any individual AIM pair while maintaining high specificity. We did not observe a clear benefit of multiplexing these markers for CD8^{+} T cells, as most of the signal was provided by the CD69^{+}4-1BB^{+} combination. These findings were consistent for immune responses to viral infections (HIV and CMV) and vaccines (SARS-CoV-2). We found CD40L to be enriched in CXCR5^{+} CD4^{+} T cells and OX40 in CCR6^{+} CD4^{+} T cells. Consequently, a slightly skewed phenotypic portrait of HIV-specific CD4^{+} T cells emerged when relying on these markers in standard AIM assays. Multiplexing the AIM assay mitigated this issue.

Our data show that the multiplexed assay has several additional advantages. It allows co-assessment of CD4^{+} and CD8^{+} T cell responses in a single panel. In contrast, in previous studies, CD4^{+} and CD8^{+} T cells were often detected by distinct single pairs of AIMs.[14,17,18,24,25] This can be deconvoluted in more standard analyses (e.g., 6xAIM Boolean OR gating vs. single AIM pair), facilitating comparisons with other studies. For instance, two studies assessing vaccine responses to distinct vaccines reported apparently conflicting results: one, using the pairs OX40^{+}4-1BB^{+} for CD4^{+} and CD69^{+}4-1BB^{+} for CD8^{+} T cells, reported that AIM^{+} responses were lower than those detected by ICS or ELISpot assays,[46] while the other one reported the opposite,[13] although it used different AIM pairs (OX40^{+}CD25^{+} and OX40^{+}PDL1^{+} for CD4^{+} and OX40^{+}CD25^{+} and CD107a^{+}CD25^{+} for CD8^{+} T cells). These discrepancies might be explained either by the antigens or by the different pairs of AIMs used, thus underlining the problematic absence of a consensual pair of AIMs. Multiplexing the assay also mitigates the donor-dependent variations observed in the specific AIM pair giving the strongest Ag-specific CD4^{+} T cell response.

One unavoidable compromise of this approach is the slightly increased background, as the background of all pairs is summed up. This could be theoretically problematic when some pair combinations do not provide any specific signal per se like in CD8^{+} T cells. Nevertheless, this had little impact on the signal-to-noise ratio that remained high in CD4^{+} T cells. Our current iteration of the multiplexed AIM assay does not provide benefit for the detection of Ag-specific CD8^{+} T cells. Alternatives are conceivable but would require the inclusion of (or substitution with) additional molecules upregulated in CD8^{+} T cells upon activation, such as PD-L1 and CD107a.[13,41,47,48] Substitution for other AIM markers could also be required for more specific purposes, like identifying T cells from lymphoid tissue where CD69 is constitutively expressed at high levels.[15]

We observed a high degree of redundancy among the AIMs in CD4^{+} T cells. For instance, when CD69, OX40, and 4-1BB markers are combined, CD40L appears to be dispensable for purely quantitative purposes—although it is a functionally important co-signaling molecule. Removing CD40L can be advantageous for some live-cell studies, as CD40L staining requires a preincubation with a CD40-blocking antibody, which might alter cellular interactions. OX40 was comparatively less redundant, further demonstrating its importance in core sets of AIM panels. Our results indicate that excluding OX40 could lead to underestimating the magnitude of responses. Therefore, redundancy in AIM markers is desirable because it mitigates possible quantitative and qualitative biases associated with individual AIM pairs.

The inclusion of multiple AIMs, each with diverse biological functions, also offers the added benefit of providing a wealth of complementary information about the functional states of the Ag-specific cells. As AIMs are functional molecules, it is not surprising that they were differentially expressed in CD4^{+} subsets. CD40L was more frequently expressed in CXCR5^{+} (Tfh-like) cells, which is consistent with studies identifying CD40L as an important co-stimulatory molecule for Tfh differentiation and function, in particular the regulation of isotype switching in B cells.[49–51] Not much is known about the role of OX40 in Th22 cells,[52] and the studies on activated Th17 cells are conflicted: on one hand, OX40 may be involved in their maintenance and functionality,[52–54] but on the other hand, the OX40-OX40L pathway would inhibit their differentiation and the production of interleukin-17 (IL-17), one of the main cytokines produced by this subset.[52,53] While the 6xAIM allows for a broader phenotyping, it still captures pathogen-specific differences in T helper differentiation, such as the elevated proportion of CXCR5^{+} and CXCR3^{+} cells in Gag-specific CD4^{+} T cells compared to CMV-specific CD4^{+} T cells.[22] Of note, removing CD40L from our analysis had a limited impact on our capacity to detect HIV-specific CXCR5^{+} CD4^{+} T cells because of the frequent redundant detection of CD40L^{+} cells by other AIM markers. In contrast, OX40 is less redundant, and its exclusion led to poor detection of HIV-specific CCR6^{+} (Th17/Th22-like) CD4^{+} T cells. Therefore, our data suggest that multiplexing the AIM assay mitigates the risk of underestimating certain CD4^{+} T cell subsets over others.

We found good consistency in the detection provided by individual pairs of AIMs across different cohorts. This further demonstrates the robustness and flexibility of the AIM assay. Yet, several individual AIM^{+} CD4^{+} T cell pairs appeared to slightly underperform in the chronic HIV infection group compared to the vaccinal cohort. Group comparisons must be analyzed with caution, as these small differences may simply reflect heterogeneity between groups of people. Alternatively, T cell dysfunction caused by persistent activation during chronic HIV infection may affect certain activation markers more than others. The multiplexed strategy can represent a harmonizing approach, as it consistently provided the highest measures of Ag-specific CD4^{+} T cells. Multiplexing the AIM can thus represent a prudent agnostic strategy when it is unknown whether a particular pathological context can have an inherent effect on individual AIM expression.

Finally, the multiplexed AIM assay could be applied to numerous vaccine studies, especially for those against HIV,

whose development remains challenging.[55] Specifically, detecting circulating Tfh (cTfh) cells in these types of studies is important, considering that they interact with B cells to help develop an efficient humoral immunity.[4] To name only a few, OX40^{+}4-1BB[+][40,56] and CD40L^{+}OX40[57] have been documented to do this in SARS-CoV-2 vaccine studies. These might not be applicable for HIV-vaccine trials, however, as we showed that the hierarchy of AIM pairs for CD4^{+} T cell detection may slightly differ between ART-treated and SARS-CoV-2-vaccinated cohorts. Instead, multiplexing the AIM assay could be a pragmatic and promising approach to optimize both the magnitude and the diversity of vaccine-induced responses detected.

Limitations of the study

We found that the multiplexed strategy, using the AIMs CD69, 4-1BB, OX40, and CD40L, was a strong alternative to using single pairs of AIMs. However, these assays were solely done on peripheral blood and do not provide a full portrait of the tissues' immune cells.[7] Although it is a reliable alternative to conventional approaches based on cytokine secretion, the AIM assay remains a functional assay. Therefore, functionally exhausted cells that do not respond to TCR stimulation will persist in being undetected. We also acknowledge that false positive events are inherent limitations of any AIM assay. This is mitigated by calculating the net responses, which is now a standard practice to analyze AIM, as it is for ICS data, but also by reporting the proportion of background signal in the raw data. As in standard AIM assays, some bystander activation can also occur in the context 6xAIM assay, but this is mitigated by selecting AIM markers less susceptible to bystander activation after a 15 h incubation.[7] The setting of the bystander activation experiment maximized the possibility of detecting bystander activation. As soluble factors can accumulate over 15 h in the "conditioned" supernatants, they are given a full extra 15 h additional incubation time to exert their non-specific activation effect (total of 30 h) instead of the standard 15 h. Additionally, this 30 h incubation extends past the 24 h, where bystander activation has been reported to take place.[7] Finally, our panel was limited to four AIMs. While CD69^{+}4-1BB^{+} proved to be a robust AIM pair to detect Ag-specific CD8^{+} T cells, the addition of other surface markers could help identify other or superior AIM combinations to characterize Ag-specific CD4^{+} and CD8^{+} T cells.

STAR★METHODS

Detailed methods are provided in the online version of this paper and include the following:

- KEY RESOURCES TABLE
- RESOURCE AVAILABILITY
  - Lead contact
  - Materials availability
  - Data and code availability
- EXPERIMENTAL MODEL AND SUBJECT DETAILS
  - Ethics statement
  - Participants and samples
- METHOD DETAILS
  - Activation-induced markers (AIM) assay
  - Bystander activation experiment
  - Software scripts and visualization
- QUANTIFICATION AND STATISTICAL ANALYSIS

AUTHOR CONTRIBUTIONS

A.L., M. Dubé, and D.E.K. designed the study; A.L., G.S., A.N., M. Dubé, M.N., G.-G.D., R.C., N.B., M.L., M. Duchesne, and A.M.S.F. performed the AIM assays; A.L. and M. Dubé analyzed the data; A.L. performed the unsupervised clustering analyses with input from O.T.; A.F. and D.E.K. secured the samples; A.L., M. Dubé, and D.E.K. wrote the initial draft of the manuscript; every author read, edited, and approved the final manuscript; and M. Dubé and D.E.K. supervised the study.

REFERENCES

1. Swain, S.L., McKinstry, K.K., and Strutt, T.M. (2012). Expanding roles for CD4+ T cells in immunity to viruses. Nat. Rev. Immunol. 12, 136–148.

2. Sant, A.J., and McMichael, A. (2012). Revealing the role of CD4+ T cells in viral immunity. J. Exp. Med. 209, 1391–1395.

3. Cox, M.A., Kahan, S.M., and Zajac, A.J. (2013). Anti-viral CD8 T cells and the cytokines that they love. Rev. Issue 435, 157–169.

4. Crotty, S. (2014). T Follicular Helper Cell Differentiation, Function, and Roles in Disease. Immunity 41, 529–542.

5. Zhu, X., and Zhu, J. (2020). CD4 T Helper Cell Subsets and Related Human Immunological Disorders. Int. J. Mol. Sci. 21, 8011.

6. Chatzileontiadou, D.S.M., Sloane, H., Nguyen, A.T., Gras, S., and Grant, E.J. (2020). The Many Faces of CD4+ T Cells: Immunological and Structural Characteristics. Int. J. Mol. Sci. 22, 73.

7. Reiss, S., Baxter, A.E., Cirelli, K.M., Dan, J.M., Morou, A., Daigneault, A., Brassard, N., Silvestri, G., Routy, J.-P., Havenar-Daughton, C., et al. (2017). Comparative analysis of activation induced marker (AIM) assays

for sensitive identification of antigen-specific CD4 T cells. PLoS One *12*, e0186998.

8. Chattopadhyay, P.K., Yu, J., and Roederer, M. (2005). A live-cell assay to detect antigen-specific CD4+ T cells with diverse cytokine profiles. Nat. Med. *11*, 1113–1117.

9. Lamoreaux, L., Roederer, M., and Koup, R. (2006). Intracellular cytokine optimization and standard operating procedure. Nat. Protoc. *1*, 1507–1516.

10. Yu, D., Rao, S., Tsai, L.M., Lee, S.K., He, Y., Sutcliffe, E.L., Srivastava, M., Linterman, M., Zheng, L., Simpson, N., et al. (2009). The Transcriptional Repressor Bcl-6 Directs T Follicular Helper Cell Lineage Commitment. Immunity *31*, 457–468.

11. Kroenke, M.A., Eto, D., Locci, M., Cho, M., Davidson, T., Haddad, E.K., and Crotty, S. (2012). Bcl6 and Maf Cooperate To Instruct Human Follicular Helper CD4 T Cell Differentiation. J. Immunol. *188*, 3734–3744.

12. Bacher, P., and Scheffold, A. (2013). Flow-cytometric analysis of rare antigen-specific T cells. Cytometry A. *83*, 692–701.

13. Bowyer, G., Rampling, T., Powlson, J., Morter, R., Wright, D., Hill, A.V.S., and Ewer, K.J. (2018). Activation-induced Markers Detect Vaccine-Specific CD4+ T Cell Responses Not Measured by Assays Conventionally Used in Clinical Trials. Vaccines *6*.

14. Ferragut, F., Cruz, K.M., Gallardo, J.P., Fernández, M., Hernández Vasquez, Y., and Gómez, K.A. (2023). Activation-induced marker assays for identification of Trypanosoma cruzi-specific CD4 or CD8 T cells in chronic Chagas disease patients. Immunology *169*, 185–203.

15. Havenar-Daughton, C., Reiss, S.M., Carnathan, D.G., Wu, J.E., Kendric, K., Torrents de la Peña, A., Kasturi, S.P., Dan, J.M., Bothwell, M., Sanders, R.W., et al. (2016). Cytokine-Independent Detection of Antigen-Specific Germinal Center T Follicular Helper Cells in Immunized Nonhuman Primates Using a Live Cell Activation-Induced Marker Technique. J. Immunol. *197*, 994–1002.

16. Frentsch, M., Arbach, O., Kirchhoff, D., Moewes, B., Worm, M., Rothe, M., Scheffold, A., and Thiel, A. (2005). Direct access to CD4+ T cells specific for defined antigens according to CD154 expression. Nat. Med. *11*, 1118–1124.

17. Painter, M.M., Mathew, D., Goel, R.R., Apostolidis, S.A., Pattekar, A., Kuthuru, O., Baxter, A.E., Herati, R.S., Oldridge, D.A., Gouma, S., et al. (2021). Rapid induction of antigen-specific CD4+ T cells is associated with coordinated humoral and cellular immunity to SARS-CoV-2 mRNA vaccination. Immunity *54*, 2133–2142.e3.

18. Goel, R.R., Painter, M.M., Apostolidis, S.A., Mathew, D., Meng, W., Rosenfeld, A.M., Lundgreen, K.A., Reynaldi, A., Khoury, D.S., Pattekar, A., et al. (2021). mRNA vaccines induce durable immune memory to SARS-CoV-2 and variants of concern. Science *374*, abm0829.

19. Dan, J.M., Lindestam Arlehamn, C.S., Weiskopf, D., da Silva Antunes, R., Havenar-Daughton, C., Reiss, S.M., Brigger, M., Bothwell, M., Sette, A., and Crotty, S. (2016). A Cytokine-Independent Approach To Identify Antigen-Specific Human Germinal Center T Follicular Helper Cells and Rare Antigen-Specific CD4+ T Cells in Blood. J. Immunol. *197*, 983–993.

20. Barham, M.S., Whatney, W.E., Khayumbi, J., Ongalo, J., Sasser, L.E., Campbell, A., Franczek, M., Kabongo, M.M., Ouma, S.G., Hayara, F.O., et al. (2020). Activation-Induced Marker Expression Identifies Mycobacterium tuberculosis–Specific CD4 T Cells in a Cytokine-Independent Manner in HIV-Infected Individuals with Latent Tuberculosis. ImmunoHorizons *4*, 573–584.

21. Morou, A., Brunet-Ratnasingham, E., Dubé, M., Charlebois, R., Mercier, E., Darko, S., Brassard, N., Nganou-Makamdop, K., Arumugam, S., Gendron-Lepage, G., et al. (2019). Altered differentiation is central to HIV-specific CD4+ T cell dysfunction in progressive disease. Nat. Immunol. *20*, 1059–1070.

22. Niessl, J., Baxter, A.E., Morou, A., Brunet-Ratnasingham, E., Sannier, G., Gendron-Lepage, G., Richard, J., Delgado, G.-G., Brassard, N., Turcotte, I., et al. (2020). Persistent expansion and Th1-like skewing of HIV-specific circulating T follicular helper cells during antiretroviral therapy. EBioMedicine *54*, 102727.

23. Brunet-Ratnasingham, E., Morou, A., Dubé, M., Niessl, J., Baxter, A.E., Tastet, O., Brassard, N., Ortega-Delgado, G., Charlebois, R., Freeman, G.J., et al. (2022). Immune checkpoint expression on HIV-specific CD4+ T cells and response to their blockade are dependent on lineage and function. EBioMedicine *84*, 104254.

24. Busà, R., Sorrentino, M.C., Russelli, G., Amico, G., Miceli, V., Miele, M., Di Bella, M., Timoneri, F., Gallo, A., Zito, G., et al. (2022). Specific Anti-SARS-CoV-2 Humoral and Cellular Immune Responses After Booster Dose of BNT162b2 Pfizer-BioNTech mRNA-Based Vaccine: Integrated Study of Adaptive Immune System Components. Front. Immunol. *13*, 856657.

25. Pallikkuth, S., Williams, E., Pahwa, R., Hoffer, M., and Pahwa, S. (2021). Association of Flu specific and SARS-CoV-2 specific CD4 T cell responses in SARS-CoV-2 infected asymptomatic heath care workers. Vaccine *39*, 6019–6024.

26. Naaber, P., Tserel, L., Kangro, K., Sepp, E., Jürjenson, V., Adamson, A., Haljasmägi, L., Rumm, A.P., Maruste, R., Kärner, J., et al. (2021). Dynamics of antibody response to BNT162b2 vaccine after six months: a longitudinal prospective study. Lancet Reg. Health. Eur. *10*, 100208.

27. Tarke, A., Coelho, C.H., Zhang, Z., Dan, J.M., Yu, E.D., Methot, N., Bloom, N.I., Goodwin, B., Phillips, E., Mallal, S., et al. (2022). SARS-CoV-2 vaccination induces immunological T cell memory able to cross-recognize variants from Alpha to Omicron. Cell *185*, 847–859.e11.

28. Grifoni, A., Weiskopf, D., Ramirez, S.I., Mateus, J., Dan, J.M., Moderbacher, C.R., Rawlings, S.A., Sutherland, A., Premkumar, L., Jadi, R.S., et al. (2020). Targets of T Cell Responses to SARS-CoV-2 Coronavirus in Humans with COVID-19 Disease and Unexposed Individuals. Cell *181*, 1489–1501.e15.

29. Rydyznski Moderbacher, C., Ramirez, S.I., Dan, J.M., Grifoni, A., Hastie, K.M., Weiskopf, D., Belanger, S., Abbott, R.K., Kim, C., Choi, J., et al. (2020). Antigen-Specific Adaptive Immunity to SARS-CoV-2 in Acute COVID-19 and Associations with Age and Disease Severity. Cell *183*, 996–1012.e19.

30. Tauzin, A., Nayrac, M., Benlarbi, M., Gong, S.Y., Gasser, R., Beaudoin-Bussières, G., Brassard, N., Laumaea, A., Vézina, D., Prévost, J., et al. (2021). A single dose of the SARS-CoV-2 vaccine BNT162b2 elicits Fc-mediated antibody effector functions and T cell responses. Cell Host Microbe *29*, 1137–1150.e6.

31. Nayrac, M., Dubé, M., Sannier, G., Nicolas, A., Marchitto, L., Tastet, O., Tauzin, A., Brassard, N., Lima-Barbosa, R., Beaudoin-Bussières, G., et al. (2022). Temporal associations of B and T cell immunity with robust vaccine responsiveness in a 16-week interval BNT162b2 regimen. Cell Rep. *39*, 111013.

32. Nicolas, A., Sannier, G., Dubé, M., Nayrac, M., Tauzin, A., Painter, M.M., Goel, R.R., Laporte, M., Gendron-Lepage, G., Medjahed, H., et al. (2023). An extended SARS-CoV-2 mRNA vaccine prime-boost interval enhances B cell immunity with limited impact on T cells. iScience *26*, 105904.

33. Sannier, G., Nicolas, A., Dubé, M., Marchitto, L., Nayrac, M., Tastet, O., Chatterjee, D., Tauzin, A., Lima-Barbosa, R., Laporte, M., et al. (2023). A third SARS-CoV-2 mRNA vaccine dose in people receiving hemodialysis overcomes B cell defects but elicits a skewed CD4+ T cell profile. Cell Rep. Med. *4*, 100955.

34. Dubé, M., Tastet, O., Dufour, C., Sannier, G., Brassard, N., Delgado, G.-G., Pagliuzza, A., Richard, C., Nayrac, M., Routy, J.-P., et al. (2023). Spontaneous HIV expression during suppressive ART is associated with the magnitude and function of HIV-specific CD4+ and CD8+ T cells. Cell Host Microbe *31*, 1507–1522.e5.

35. Daoussis, D., Andonopoulos, A.P., and Liossis, S.N.C. (2004). Targeting CD40L: a Promising Therapeutic Approach. Clin. Diagn. Lab. Immunol. *11*, 635–641.

36. Croft, M., So, T., Duan, W., and Soroosh, P. (2009). The significance of OX40 and OX40L to T-cell biology and immune disease. Immunol. Rev. *229*, 173–191.

37. Fu, N., Xie, F., Sun, Z., and Wang, Q. (2021). The OX40/OX40L Axis Regulates T Follicular Helper Cell Differentiation: Implications for Autoimmune Diseases. Front. Immunol. *12*, 670637.

38. Lachmann, R., Bajwa, M., Vita, S., Smith, H., Cheek, E., Akbar, A., and Kern, F. (2012). Polyfunctional T Cells Accumulate in Large Human Cytomegalovirus-Specific T Cell Responses. J. Virol. *86*, 1001–1009.

39. Sonnet, F., Namork, E., Stylianou, E., Gaare-Olstad, I., Huse, K., Andorf, S., Mjaaland, S., Dirven, H., and Nygaard, U. (2020). Reduced polyfunctional T cells and increased cellular activation markers in adult allergy patients reporting adverse reactions to food. BMC Immunol. *21*, 43.

40. Thieme, C.J., Anft, M., Paniskaki, K., Blazquez-Navarro, A., Doevelaar, A., Seibert, F.S., Hoelzer, B., Konik, M.J., Berger, M.M., Brenner, T., et al. (2020). Robust T Cell Response Toward Spike, Membrane, and Nucleocapsid SARS-CoV-2 Proteins Is Not Associated with Recovery in Critical COVID-19 Patients. Cell Rep. Med. *1*, 100092.

41. Niessl, J., Baxter, A.E., Mendoza, P., Jankovic, M., Cohen, Y.Z., Butler, A.L., Lu, C.-L., Dubé, M., Shimeliovich, I., Gruell, H., et al. (2020). Combination anti-HIV-1 antibody therapy is associated with increased virus-specific T cell immunity. Nat. Med. *26*, 222–227.

42. Lichtner, M., Cicconi, P., Vita, S., Cozzi-Lepri, A., Galli, M., Lo Caputo, S., Saracino, A., De Luca, A., Moioli, M., Maggiolo, F., et al. (2015). Cytomegalovirus Coinfection Is Associated With an Increased Risk of Severe Non–AIDS-Defining Events in a Large Cohort of HIV-Infected Patients. J. Infect. Dis. *211*, 178–186.

43. Booiman, T., Wit, F.W., Girigorie, A.F., Maurer, I., De Francesco, D., Sabin, C.A., Harskamp, A.M., Prins, M., Franceschi, C., Deeks, S.G., et al. (2017). Terminal differentiation of T cells is strongly associated with CMV infection and increased in HIV-positive individuals on ART and lifestyle matched controls. PLoS One *12*, e0183357.

44. Becht, E., McInnes, L., Healy, J., Dutertre, C.-A., Kwok, I.W.H., Ng, L.G., Ginhoux, F., and Newell, E.W. (2018). Dimensionality reduction for visualizing single-cell data using UMAP. Nat. Biotechnol. *37*, 38–44.

45. Levine, J.H., Simonds, E.F., Bendall, S.C., Davis, K.L., Amir, E.a.D., Tadmor, M.D., Litvin, O., Fienberg, H.G., Jager, A., Zunder, E.R., et al. (2015). Data-Driven Phenotypic Dissection of AML Reveals Progenitor-like Cells that Correlate with Prognosis. Cell *162*, 184–197.

46. Tan, A.T., Lim, J.M., Le Bert, N., Kunasegaran, K., Chia, A., Qui, M.D., Tan, N., Chia, W.N., de Alwis, R., Ying, D., et al. (2021). Rapid measurement of SARS-CoV-2 spike T cells in whole blood from vaccinated and naturally infected individuals. J. Clin. Invest. *131*, e152379.

47. Betts, M.R., Brenchley, J.M., Price, D.A., De Rosa, S.C., Douek, D.C., Roederer, M., and Koup, R.A. (2003). Sensitive and viable identification of antigen-specific CD8+ T cells by a flow cytometric assay for degranulation. J. Immunol. Methods *281*, 65–78.

48. Wolint, P., Betts, M.R., Koup, R.A., and Oxenius, A. (2004). Immediate Cytotoxicity But Not Degranulation Distinguishes Effector and Memory Subsets of CD8+ T Cells. J. Exp. Med. *199*, 925–936.

49. Deenick, E.K., and Ma, C.S. (2011). The regulation and role of T follicular helper cells in immunity. Immunology *134*, 361–367.

50. Awe, O., Hufford, M.M., Wu, H., Pham, D., Chang, H.-C., Jabeen, R., Dent, A.L., and Kaplan, M.H. (2015). PU.1 Expression in T Follicular Helper Cells Limits CD40L-Dependent Germinal Center B Cell Development. J. Immunol. *195*, 3705–3715.

51. Cicalese, M.P., Gerosa, J., Baronio, M., Montin, D., Licciardi, F., Soresina, A., Dellepiane, R.M., Miano, M., Baselli, L.A., Volpi, S., et al. (2018). Circulating Follicular Helper and Follicular Regulatory T Cells Are Severely Compromised in Human CD40 Deficiency: A Case Report. Front. Immunol. *9*, 1761.

52. Fu, Y., Lin, Q., Zhang, Z., and Zhang, L. (2020). Therapeutic strategies for the costimulatory molecule OX40 in T-cell-mediated immunity. Acta Pharm. Sin. B *10*, 414–433.

53. Furue, M., and Furue, M. (2021). OX40L–OX40 Signaling in Atopic Dermatitis. J. Clin. Med. *10*, 2578.

54. Zhang, Z., Zhong, W., Hinrichs, D., Wu, X., Weinberg, A., Hall, M., Spencer, D., Wegmann, K., and Rosenbaum, J.T. (2010). Activation of OX40 Augments Th17 Cytokine Expression and Antigen-Specific Uveitis. Am. J. Pathol. *177*, 2912–2920.

55. Haynes, B.F., Wiehe, K., Borrow, P., Saunders, K.O., Korber, B., Wagh, K., McMichael, A.J., Kelsoe, G., Hahn, B.H., Alt, F., and Shaw, G.M. (2023). Strategies for HIV-1 vaccines that induce broadly neutralizing antibodies. Nat. Rev. Immunol. *23*, 142–158.

56. Mise-Omata, S., Ikeda, M., Takeshita, M., Uwamino, Y., Wakui, M., Arai, T., Yoshifuji, A., Murano, K., Siomi, H., Nakagawara, K., et al. (2022). Memory B Cells and Memory T Cells Induced by SARS-CoV-2 Booster Vaccination or Infection Show Different Dynamics and Responsiveness to the Omicron Variant. J. Immunol. *209*, 2104–2113.

57. Rydyznski Moderbacher, C., Kim, C., Mateus, J., Plested, J., Zhu, M., Cloney-Clark, S., Weiskopf, D., Sette, A., Fries, L., Glenn, G., and Crotty, S. (2022). NVX-CoV2373 vaccination induces functional SARS-CoV-2–specific CD4+ and CD8+ T cell responses. J. Clin. Invest. *132*, e160898.

58. Ellis, B., Haaland, P., Florian, H., Le Meur, N., Gopalakrishnan, N., Spidlen, J., Jiang, M., Finak, G., and Grandjeaud, S. (2022). flowCore: Basic Structures for Flow Cytometry Data.

59. Quintelier, K., Couckuyt, A., Emmaneel, A., Aerts, J., Saeys, Y., and Van Gassen, S. (2021). Analyzing high-dimensional cytometry data using Flow-SOM. Nat. Protoc. *16*, 3775–3801.

60. John, C.R., Watson, D., Russ, D., Goldmann, K., Ehrenstein, M., Pitzalis, C., Lewis, M., and Barnes, M. (2020). M3C: Monte Carlo reference-based consensus clustering. Sci. Rep. *10*, 1816.

61. Wickham, H. (2016). ggplot2: Elegant Graphics for Data Analysis.

62. Kolde, R. (2019). Pheatmap: Pretty Heatmaps.

63. Bion, R. ggradar: Create Radar Charts Using Ggplot2

Cell Reports Methods
Article

STAR★METHODS

KEY RESOURCES TABLE

REAGENT or RESOURCE	SOURCE	IDENTIFIER
Antibodies		
G025H7 (BV605) [Human anti-CD183 (CXCR3)]	Biolegend	Cat#353728; Lot:B323111; RRID:AB_2563157
J25D4 (BV421) [Human anti-CD185 (CXCR5)]	Biolegend	Cat#356920; Lot:B340671; RRID:AB_2562303
13B 1E5 (BUV805) [Human anti-CD186 (CXCR6)]	BD Biosciences	Cat#748448; Lot:2104048; RRID:AB_2872864
11A9 (BUV737) [Human anti-CD196 (CCR6)]	BD Biosciences	Cat#612780; Lot:1256027; RRID:AB_2870109
UCHT1 (BUV496) [Human anti-CD3]	BD Biosciences	Cat#612940; Lot:1347983; RRID:AB_2870222
SK3 (BB630) [Human anti-CD4]	BD Biosciences	Cat#624294 CUSTOM; Lot:1203097
RPA-T8 (BV570) [Human anti-CD8]	Biolegend	Cat#301038; Lot:B333843; RRID:AB_2563213
M5E2 (BV480) [Human anti-CD14]	BD Biosciences	Cat#746304; Lot:2139313; RRID:AB_2743629
HIB19 (BV480) [Human anti-CD19]	BD Biosciences	Cat#746457; Lot:2123638; RRID:AB_2743759
HIT2 (BB790) [Human anti-CD38]	BD Biosciences	Cat#624296 CUSTOM; Lot:2242331
HI100 (PerCP Cy5.5) [Human anti-CD45RA]	BD Biosciences	Cat#563429; Lot:0223218; RRID:AB_2738199
FN50 (BV650) [Human anti-CD69]	Biolegend	Cat#310934; Lot:B364649; RRID:AB_2563158
ACT35 (APC) [Human anti-CD134 (OX40)]	BD Biosciences	Cat#563473; Lot:1015537; RRID:AB_2738230
4B4-1 (PE-Dazzle 594) [Human anti-CD137 (4-1BB)]	Biolegend	Cat#309826; Lot:B349385; RRID:AB_2566260
TRAP1 (PE) [Human anti-CD154 (CD40L)]	BD Biosciences	Cat#555700; Lot:7086896; RRID:AB_396050
EH122H (BV711) [Human anti-CD279 (PD-1)]	Biolegend	Cat#329928; Lot:B366791; RRID:AB_2562911
LN3 (FITC) [Human anti-HLA-DR]	Biolegend	Cat#327006; Lot:B359252; RRID:AB_893569
CD40-blocking antibody	Miltenyi Biotec	Cat#130-094-133
LIVE/DEAD Fixable dead cell	Thermo Fisher Scientific	Lot:L34960
Biological samples		
HIV ART-treated donor blood samples	N/A	
SARS-CoV-2 naive donor blood samples	N/A	
Chemicals, peptides, and recombinant proteins		
Roswell Park Memorial Institute (RPMI)	Thermo Fischer Scientific	Cat#61870036
HEPES	Thermo Fischer Scientific	Cat#15630-080
Penicillin/Streptomycin	VWR	Cat#450-201-EL
Fetal Bovine Serum (FBS)	VWR	Cat#97068-085
PepMix™ SARS-CoV-2 (Spike Glycoprotein)	JPT	Cat#PM-WCPV-S-1
PepMix™ HIV-1 (GAG) Ultra	JPT	Cat#PM-HIV-GAG
PepMix™ HIV-1 (POL) Ultra	JPT	Cat#PM-HIV-POL
PepMix™ HIV-1 (ENV) Ultra	JPT	Cat#PM-HIV-ENV
PepMix™ HIV-1 (NEF) Ultra	JPT	Cat#PM-HIV-NEF
PepMix™ HCMVA (pp65)	JPT	Cat#PM-PP65-1
Staphylococcal Enterotoxin B (SEB)	Toxin technology	Cat#BT202
Software and algorithms		
FlowJo v10.8.2	FlowJo LLC	https://www.flowjo.com/
R v4.2.2	R Core Team	https://www.r-project.org/
RStudio v2023.03.1 + 446	RStudio	https://posit.co/download/rstudio-desktop
R scripts	https://github.com/alemi055/scripts-and-data/tree/master, in the archive Lemieuxetal_CellRepMet_2024.tar.bz2	https://doi.org/10.5281/zenodo.10465085

RESOURCE AVAILABILITY

Lead contact
Further information and requests for resources and reagents should be directed to and will be fulfilled by the lead contact, Daniel E. Kaufmann (daniel.kaufmann@chuv.ch).

Materials availability
There are restrictions to the availability of clinical samples (PBMCs), in compliance with our IRB protocols and the informed consent obtained from each participant. This study did not generate new unique reagents.

Data and code availability
- The published article includes all of the processed datasets generated for this study. Further information and requests for resources and reagents should be directed to and fulfilled by the Lead contact Author (daniel.kaufmann@chuv.ch).
- We developed R codes scripted to create spider charts and perform unsupervised analyses on HIV-specific CD4+ T cells. All original codes have been deposited at Github and are publicly available as of publication. DOIs are listed in the key resources table.
- Any additional information required to reanalyze the data reported in this paper is available from the Lead contact Author upon request (daniel.kaufmann@chuv.ch).

EXPERIMENTAL MODEL AND SUBJECT DETAILS

Ethics statement
All work was conducted in accordance with the Declaration of Helsinki in terms of informed consent and approval by an appropriate institutional board. Blood samples were obtained from donors who consented to participate in this research project at the CHUM (13.019 and 19.381). Plasma and PBMCs were isolated by centrifugation and Ficoll gradient, and samples were stored at $-80°C$ and in liquid nitrogen, respectively, until use.

Participants and samples
We obtained the leukaphereses from study participants at the McGill University Health Center (Montréal, QC, Canada), and at the Center Hospitalier de l'Université de Montréal (CHUM; Montréal, QC, Canada). The study was approved by the respective IRBs, and written informed consent was obtained from all participants before enrollment. Our cohort of 16 ART-treated participants[34] with controlled viremia (<40 viral RNA copies/mL) was used to measure HIV and CMV-specific responses. One donor who was negative for CMV was removed from the CMV analyses. The SARS-CoV-2 vaccinated cohort included 23 healthcare workers (HCW) who had never been previously infected by the virus and received two doses of mRNA vaccine, with a 16-week interval. Blood samples were collected approximately three weeks after the second dose. The number of participants for this specific time point was the same as previously published.[31] The characteristics of all participants are summarized in Table S1. PBMCs were isolated by the Ficoll density gradient method and stored in liquid nitrogen until use.

METHOD DETAILS

Activation-induced markers (AIM) assay
The multiplexed AIM assay[21–23,41] was adapted for HIV-,[34] CMV-, and SARS-CoV-2-specific[30–33] CD4+ and CD8+ T cells. PBMCs were thawed and rested for 3 h in 96-well flat-bottom plates in RPMI 1640 supplemented with HEPES, penicillin/streptomycin, and 10% FBS. For HIV, 2×10^6 PBMCs were stimulated with pools of 150 overlapping peptides of HIV-1 Gag, Pol, Env, or Nef proteins (0.5 μg/mL per peptide) (JPT) for 15 h (37°C, 5% CO₂). For CMV, 2×10^6 PBMCs were also stimulated with a pool of 138 overlapping HCMVA 65 kDa phosphoprotein (pp65) (0.5 μg/mL per peptide) (JPT) peptides. For SARS-CoV-2, the stimulation was done with 1.7×10^6 PBMCs and an S glycoprotein peptide pool (0.5 μg/mL per peptide), corresponding to the pool of 315 overlapping peptides (15-mers) spanning the complete amino acid sequence of the Spike Glycoprotein (JPT). CCR6, CXCR3, CXCR5, and CXCR6 antibodies, as well as a CD40 blocking antibody, were added in culture 15 min before stimulation. A DMSO-treated condition and a *Staphylococcus enterotoxin B* (SEB)-treated (0.5 μg/mL) condition served, respectively, as negative and positive controls. Cells were first stained for viability dye (Aquavivid, Thermofisher, 20 min, 4°C), surface markers (30 min, 4°C) (see Table S2 for the list of antibodies), and then fixed using 1% paraformaldehyde (15 min, 4°C) before acquisition on the flow cytometer FACSymphony A5 Cell Analyzer (BD Biosciences). Figure S1A describes the upstream gating strategy. Analyses were performed using FlowJo (v10.8.2).

Bystander activation experiment
A first AIM assay [AIM #1] was performed, as described above, on PBMCs of three ART participants thawed on day 1. On day 2, after 15 h of Gag stimulation, the conditioned supernatants from this AIM #1 were collected, clarified by two rounds of centrifugation (at 900 RPM and 1500 RPM, respectively, for 10 min each) in 1.5 mL microtubes, then transferred on freshly purified CD3+ T lymphocytes

(negative selection with the EasySep Human T cell Isolation Kit; StemCell) from an HIV-naïve participant (uninfected donor, UD) [AIM #2]. These "sentinel" T cells were incubated for 15 h in the conditioned supernatants and stained on day 3. Cells from AIM #1 and AIM #2 were acquired on the FACSymphony A5 Cell Analyzer on days 2 and 3, respectively.

Software scripts and visualization

Graphics were generated using GraphPad PRISM (v9.5.0) (GraphPad, San Diego, CA). For the unsupervised analyses, HIV-specific $CD4^+$ T cells were first downsampled to a comparable number of events (500 cells), and FCS files were loaded through the flowCore package (v2.10.0).[58] Scaling and logicle transformation of the flow cytometry data was applied using FlowSOM (v2.6.0),[59] as done previously.[31] The uniform manifold approximation and projection (UMAP) algorithm was performed using the R package M3C (v1.20.0),[60] while the clustering was achieved using Phenograph (v0.99.1)[45] with the k parameter (number of nearest-neighbors) set to 250, which we determined based on numerous iterations with varying k values until this plateau was reached. We obtained 12 clusters. These clusters were further grouped in "superclusters" based on their similar patterns of polarization markers expression. Heatmaps and spider charts were generated in R (v4.2.2) using the packages gglot2 (v3.4.0),[61] pheatmap (v1.0.12),[62] and ggradar (v0.2).[63] R codes scripted for this paper are available at https://github.com/alemi055/scripts-and-data/tree/master, in the archive Lemieuxetal_CellRepMet_2024.tar.bz2.

QUANTIFICATION AND STATISTICAL ANALYSIS

Antigen-specific T cell responses are expressed in percentages of $CD4^+$ and $CD8^+$ T cells. Symbols (circles for the HIV cohort, squares for the CMV cohort, and triangles for the SARS-CoV-2 cohort) represent biologically independent samples. Lines connect data from the same donor. Median fold increases (FIs) were calculated by dividing the net T cell responses of the 6xAIM by the individual AIM pair's (net FIs), or the AIM^+ T cell responses of each pair by its respective unstimulated (background) values (raw FIs). For the intra- and inter-experiment reproducibility, coefficients of variation (CV) were calculated by dividing the standard deviation by the mean. Differences in responses for the same donor in the HIV and CMV cohorts were performed using Wilcoxon matched pair tests, while tests comparing different donors in the HIV and SARS-CoV-2 cohorts were performed using Mann-Whitney (unpaired) tests. Pairwise multiple comparisons were performed using the Friedman test with Dunn's post-hoc test. The Wilcoxon, Mann-Whitney, and Friedman tests were generated using GraphPad Prism. p values are indicated for each comparison assessed, and $p < 0.05$ were considered significant. For graphical representation on a log scale (but not for statistical tests), null values were arbitrarily set at the minimal values for each assay.